Micellization of Poly(ethylene oxide)–Poly(propylene oxide) Block Copolymer in Aqueous Solution: Effect of Polymer Impurities

Per Linse

Physical Chemistry 1, Chemical Center, University of Lund, P.O. Box 124, S-221 00 Lund, Sweden

Received November 8, 1993; Revised Manuscript Received February 18, 1994[⊕]

ABSTRACT: The effect of polymer impurities on the micellization in aqueous solutions of a PEO–PPO–PEO triblock copolymer [PEO and PPO are poly(ethylene oxide) and poly(propylene oxide), respectively] was modeled with a mean-field lattice theory for multicomponent mixtures of copolymers with internal states occurring in heterogeneous systems. A PEO–PPO diblock copolymer and PEO and PPO homopolymers were considered as impurities. The critical micellar concentration (cmc), the aggregation number, and the fraction of impurities as well as the spatial distribution of segments in the micelle have been investigated. In particular, the presence of the diblock impurity reduces the cmc and increases the aggregation number. At the cmc, the diblock impurity aggregates more readily than the triblock copolymer, and the fraction of the impurity in the micelles could be a factor of 4 larger than the stoichiometric fraction. The width of the PO/EO interface in the micelles was not affected by the presence of the diblock impurity. The PPO homopolymer also reduces the cmc but to a lesser extent. The existence of polymer micelles increases the solubility of PPO by several orders of magnitude by solubilization of PPO in the hydrophobic core of the micelle. Despite the low solubility of PPO in aqueous solution, ca. 10% of the micellear volume could consist of solubilized PPO. The amount of PPO solubilized per micelle increases strongly with temperature and with the volume fraction of free PPO but only weakly with the volume fraction of the triblock copolymer. The effect of the PEO impurity on the micellization was negligible. It was also concluded that the repulsive interaction among the PEO headgroups determines the growth of the micelles.

I. Introduction

Triblock copolymers of the PEO–PPO–PEO type [PEO and PPO are poly(ethylene oxide) and poly(propylene oxide), respectively], often referred to as Pluronic polymers, have been a subject of great interest during recent years.[1-9] The self-association phenomenon due to the more hydrophobic PPO block and the more hydrophilic PEO block forms the basis for many applications of the Pluronic polymers. In addition to the extensive experimental investigation, some theoretical studies of micellization,[10-12] solubilization,[12] and phase behavior[13] have been performed.

The micellization process of Pluronic polymers is largely similar to that of smaller surfactant molecules. The critical micellar concentration (cmc), however, is less well determined, and the reported cmc and aggregation number values differ substantially due to the presence of polymer impurities[2] and to a substantial polydispersity, which are consequences of the manufacturing process.

The aim of the present investigation is to theoretically examine the influence of a small amount of PEO–PPO diblock copolymer as well as of PPO and PEO homopolymers on the micellization process. The effect of the polydispersity of the Pluronic polymers is the subject of a forthcoming report. The present study is a continuation of a previous one,[11] in which the influence of the polymer composition and structure of block copolymers containing PEO and PPO on the micellization was examined. In the former studies,[11,13] it was found that the theoretical critical micellar temperature curves were displaced by ≈20–30 K above the experimental ones and, moreover, no micellization could be predicted for the shortest polymers of the Pluronic family. It was suggested that the presence of impurities and in particular the polydispersity of the experimental samples contribute to this discrepancy.

The theoretical description is based on a lattice theory for heterogeneous systems, initially developed by Scheutjens and Fleer[14] and later extended for the description of micelle formation[15] and polymers possessing internal degrees of freedom.[16] The latter approach provides us with a formalism where temperature- and concentration-dependent interaction parameters can be obtained by using a conformational model.[17] Such a polymer model has successfully been used for describing the inverse temperature behavior of aqueous solutions of PEO and related polymers (a worsening of the solvency condition occurs on increasing temperature, eventually leading to phase separation). The conformational model accounts for the fact that different conformations of ethylene oxide groups differ in their dipole moments and that the polar conformations are less numerous. The conformations are divided into two classes or states, one being more polar with a low energy and a low statistical weight and one being less polar (referred to as nonpolar) with a higher energy and a higher statistical weight. At low temperatures, the former class is dominating and the effective polymer–solvent interaction is favorable, whereas at higher temperatures, the latter class is more important, rendering the polymer–solvent interaction more unfavorable. Furthermore, the effective polymer–solvent interaction becomes more unfavorable as the polymer concentration increases.

II. Theory

The theoretical approach embraces a determination of whether the Pluronic polymers in an aqueous solution form micelles or remain unaggregated. The conditions for the existence of stable aggregates and their size and composition were examined by using a lattice theory for multicomponent mixtures of copolymers with internal degrees of freedom.[16] Since the theory and the set of interaction parameters used are the same as those in the previous investigation of micellization of Pluronic polymers,[11] only

[⊕] Abstract published in *Advance ACS Abstracts,* April 1, 1994.

0024-9297/94/2227-2685$04.50/0

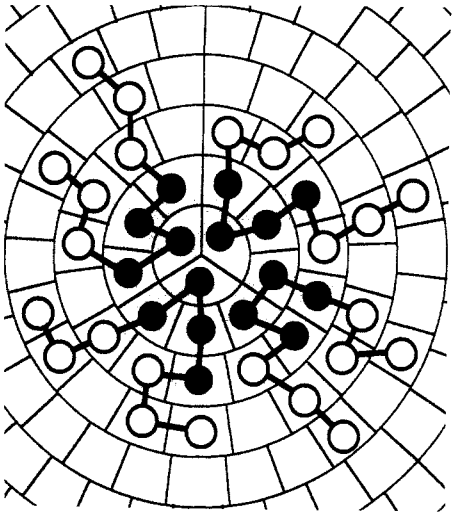

Figure 1. Two-dimensional illustration of an infinite spherical lattice and a micelle formed by four triblock copolymers, $B_3A_4B_3$. The hydrophobic segments A (filled circles) form the central part of the micelle, whereas the more hydrophilic segments B (open circles) form the outer layer of the micelle. Note the small number of unfavorable contacts between the hydrophobic segments and the solvent (unfilled lattice cells).

a brief account, adapted for calculations of multicomponent micelles, is given here. For a more detailed description of the lattice theory, see e.g., refs 14–16.

The space is divided into concentric shells, and each shell is further divided into lattice cells, each containing one polymer segment or a solvent molecule. The conformations of a polymer chain are described as random walks on the spherical lattice; see Figure 1. The interaction extends only to segments or solvent molecules in adjacent lattice cells. The random-mixing (mean-field) approximation is applied within each layer separately, and thus we are able to obtain and describe radial concentration profiles.

The computation involves a self-consistent determination of the *state* distribution (i.e., the distributions of the polar and nonpolar states of the EO and PO species in each layer) and the *segment* distribution (i.e., the radial distribution of each polymer segment and of water molecules). The state distribution is derived from the partition function and is given by the following implicit set of nonlinear equations[16]

$$P_{ABi} = \frac{X_{AB}}{\sum_B X_{AB}},$$

$$X_{AB} \equiv g_{AB} \exp[-\beta U_{AB} - \sum_{A'}\sum_{B'} \chi_{BB'} \langle P_{A'B'i}\phi_{A'i}\rangle] \quad (1)$$

valid for all species (EO, PO, and water, collectively labeled A), states (polar and nonpolar conformations in the case of EO or PO, collectively labeled B), and layers (i). In eq 1, P_{ABi} denotes the fraction of species A in layer i which is in state B, U_{AB} the internal energy of state B of species A (arising from different internal energies between the polar and nonpolar conformations), g_{AB} the degeneration factor of state B of species A (arising from different numbers of polar and nonpolar conformations), $\chi_{BB'}$ the Flory–Huggins interaction parameter representing the interaction between species A in state B and species A′ in state B′, and ϕ_{Ai} the volume fraction of species A in layer i. Moreover, $\beta = (kT)^{-1}$, where k is Boltzmann's constant and T the absolute temperature. The angular brackets indicate an averaging over three adjacent layers. Thus, a state is favored by high degeneration, low internal energy, and favorable interaction (small χ) with its neighboring segments.

The species volume fraction ϕ_{Ai} needed in eq 1 is simply related to n_{xsi}, the number of sites in layer i occupied by segments of rank s (the sth segment in a chain) belonging to component x according to

$$\phi_{Ai} = \frac{1}{L_i}\sum_x \sum_{s=1}^{r_x} \delta_{A,t(x,s)} n_{xsi} \quad (2)$$

where L_i is the number of sites in layer i and r_x the number of segments in component x. The Kronecker delta selects only segments of rank s of component x if they are of type A.

The expression of the segment distribution becomes more complex since the correct weight of all conformations and the connectivity of the chains have to be taken into account. Again starting from the partition function, n_{xsi} is obtained by a matrix method and is given by[16]

$$n_{xsi} = C_x\{\Delta_i^{T}\cdot[\prod_{s'=r_x}^{s+1}(\mathbf{W}^{t(x,s')})^{T}]\cdot\mathbf{s}\}\{\Delta_i^{T}\cdot[\prod_{s'=2}^{s}\mathbf{W}^{t(x,s')}]\cdot\mathbf{p}(x,1)\} \quad (3)$$

where C_x is a normalization factor related to the bulk volume fraction of component x, $\mathbf{W}^{t(x,s)}$ a tridiagonal matrix comprising elements which contain factors describing the lattice topology and weighting factors for segments of rank s belonging to component x, and $\mathbf{p}(x,1)$ a vector describing the distribution of the first segment of component x among the layers, Δ and $\mathbf{s}$ being elementary column vectors. In the present study, a hexagonal lattice with 12 nearest neighbors has been used. The weighting factor G_{Ai} for species A in layer i entering $\mathbf{W}$ is given by

$$G_{Ai} = \exp(-\beta u_{Ai}) \quad (4)$$

where the species potential u_{Ai} can be divided into two parts according to

$$u_{Ai} = u'_i + u_{Ai}^{int} \quad (5)$$

If the species potentials are defined with respect to the bulk solution, i.e., if $u_A^b = 0$, then the two terms are given by

$$\beta u'_i \equiv \alpha_i + \sum_x \frac{\phi_x^b}{r_x} + \frac{1}{2}\sum_{A'}\sum_{A''}\sum_{B'}\sum_{B''}\phi_{A'}^b P_{A'B'}^b \chi_{B'B''} P_{A''B''}^b \phi_{A''}^b$$

$$\beta u_{Ai}^{int} \equiv \sum_B \left[P_{ABi}\left(\beta U_{AB} + \ln\frac{P_{ABi}}{g_{AB}}\right) - P_{AB}^b\left(\beta U_{AB} + \ln\frac{P_{AB}^b}{g_{AB}}\right)\right] + \sum_{A'}\sum_B\sum_{B'}\chi_{BB'}(P_{ABi}\langle P_{A'B'i}\phi_{A'i}\rangle - P_{AB}^b P_{A'B'}^b \phi_{A'}^b) \quad (6)$$

The species-independent term u'_i ensures that the space is completely filled in layer i by a suitable choice of α_i, and u'_i is related to the lateral pressure in a continuous model. In bulk u' becomes zero. The species-dependent term u_{Ai}^{int} has two contributions: the internal free energy for species A in layer i being diminished by the corresponding

quantity in bulk and the mixing energy for species A in layer i being diminished by the mixing energy for species A in bulk. In both cases, averages are taken over the relevant state distributions. At distances far away from the center of the aggregate, P_{ABi} approaches P_{AB}^{b}, ϕ_{Ai} approaches ϕ_{A}^{b}, and hence u_{Ai}^{int} becomes zero. Since u_{Ai} is needed for obtaining ϕ_{Ai} through eqs 2–4 and u_{Ai} depends itself on ϕ_{Ai} according to eqs 5 and 6, eqs 2–6 have to be solved self-consistently. At the same time, the state distribution, which depends on ϕ_{Ai}, has to fulfill eq 1.

The solution of eqs 1–6 has two branches, one corresponding to homogeneous concentration profiles throughout the entire lattice and one to a single micelle, formed at the center of the lattice, in equilibrium with the specified bulk concentration of the components. The free energy of forming the micelle at a fixed position, A^{σ}, is readily calculated from the volume fraction distributions of the species and of the states and from the chemical potentials of the components in bulk according to eqs 2–6, 14, and 15 in ref 11. At equilibrium A^{σ} (>0) is balanced by a negative mixing entropy $kT \ln(V_m/V_s)$, where V_m is the volume of the micelle and V_s is the volume of a subsystem containing one micelle and its accompanying solution.[15] The micellar volume is approximated by

$$V_m = \frac{\sum_x' \Gamma_x}{\sum_x' \phi_{x,i=1} - \sum_x' \phi_x^b} \tag{7}$$

where the prime restricts the summation to components constituting the micelle (all components except water and PEO) and Γ_x is the excess number of segments of component x in the subsystem (given by eq 16 in ref 11). The *total* volume fraction of component x in the subsystem (equal to the stoichiometric concentration of x in the micellar solution) is the sum of the excess and bulk volume fractions according to

$$\phi_x^{tot} = \frac{\Gamma_x}{V_s} + \phi_x^b \tag{8}$$

On the basis of a selected bulk composition $\{\phi_x^b\}$, the numerical procedure involves the computation of the equilibrium state and segment distributions according to eqs 1–6, and then the excess free energy of the subsystem A^{σ} and the set of the excess number of segments of the components $\{\Gamma_x\}$ are calculated. Subsequently eq 7 provides the micellar volume which together with A^{σ} and the requirement of equilibrium gives V_s. Finally, the total composition $\{\phi_x^{tot}\}$ is obtained from eq 8. Any change in the bulk composition $\{\phi_x^b\}$ leads to a change in the total composition, and the desired $\{\phi_x^{tot}\}$ was obtained by variation of $\{\phi_x^b\}$.

The aggregation number of the micelle without impurities is simply given by $N_{agg} = \Gamma_{P105}/r_{P105}$, i.e., the excess of Pluronic P105 segments divided by the number of segments of a single Pluronic P105 chain. In the case *with* impurities, an effective aggregation number is defined according to

$$N_{agg}^{eff} = \Gamma_{polymer}/r_{P105} \tag{9}$$

Since the excess of polymer segments $\Gamma_{polymer}$ is the sum of Pluronic P105 and impurity segments, N_{agg}^{eff} is the aggregation number of Pluronic P105 which would be observed *if* the occurrence of the impurities were not known.

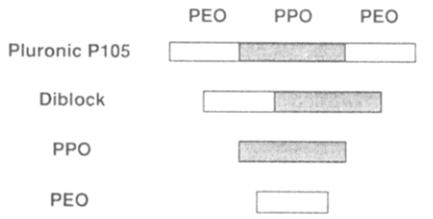

Figure 2. Schematic illustration of the molecular structure of the Pluronic P105 triblock copolymer and the polymer impurities studied. The PEO blocks are represented by open areas and the PPO blocks by shaded areas, the length of each area is proportional to the number of monomers of the block. The compositions used in the model calculations were $(EO)_{37}(PO)_{56}(EO)_{37}$, $(EO)_{37}(PO)_{56}$, $(PO)_{56}$, and $(EO)_{37}$, respectively. Pluronic is a trademark of BASF Wyandotte Chemical Corp. The composition of Pluronic P105 was calculated from data provided by the manufacturer.

Finally, in the following the bulk volume fraction of component x, ϕ_x^b, will be referred to as the free volume fraction of component x, ϕ_x^f, whereas the excess amount will be referred to as the amount being aggregated or solubilized.

III. Polymer Model

Polymers. Pluronic polymers with a broad range of total mass and of EO/PO ratio are commercially available. The synthesis procedure, however, leads to mass and composition (EO/PO ratio) distributions of the desired triblock copolymer as well as to the formation of homopolymers and diblock copolymers (referred to as impurities). A model of an aqueous solution of (monodisperse) Pluronic P105 is used for the investigation of the effects of the impurities. Figure 2 shows schematically the molecular structures of Pluronic P105 and the impurities related to it which are considered, and their compositions are given in the figure caption. Each of the blocks of the polymer impurities has the same number of segments as the corresponding block in Pluronic P105. Also very likely to occur is the corresponding diblock impurity with only half the number of PO segments. The influence of this diblock copolymer on the micellization is, however, believed to be smaller due to an unchanged EO/PO ratio as compared to the Pluronic polymer.

Interaction Parameters. In order to pursue the calculations, parameters describing the interaction among the species and the state equilibrium have to be specified. The internal state energy, U_{AB}, and the degeneration, g_{AB}, of all states of all species, as well as the Flory–Huggins interaction parameters between all pairs of species in the different states, χ_{BB}, are displayed in Table 1. All of them were previously determined for simpler systems (binary PEO/water,[17,18] binary PPO/water,[16] and ternary PEO/PPO/water solutions[19]) by fitting calculated phase diagrams to experimental ones. Thus, in the present study there are no adjustable parameters. The set of parameters is the same as those in the previous investigations of the micellization of EO and PO containing block copolymers[11] and of the phase behavior of Pluronic polymers in aqueous solution.[13]

IV. Results and Discussion

Diblock Impurity. The calculated critical micellar temperature (cmt) as a function of the polymer volume fraction for an aqueous solution of Pluronic P105 without impurity is shown in Figure 3 (dashed curve). As previously found experimentally,[1–9] as well as theoretically for

Table 1. Internal State Parameters (U_{AB} and g_{AB}) and Flory–Huggins Interaction Parameters ($\chi_{BB'}$) of the Theoretical Model (Energy in kJ mol^{-1})

state no.	species	state	U_{AB}	g_{AB}
1	water		0	1
2	EO	polar	0[a]	1[a]
3		nonpolar	5.086[a]	8[a]
4	PO	polar	0[b]	1[b]
5		nonpolar	11.5[b]	60[b]

	$kT\chi_{BB'}$			
state no.	2	3	4	5
1	0.6508[a]	5.568[a]	1.7[b]	8.5[b]
2		1.266[a]	1.8[c]	3.0[c]
3			0.5[c]	−2.0[c]
4				1.4[b]

[a] From the fit to the experimental data of the binary PEO/water phase diagram (see refs 17 and 18). [b] From the fit to the experimental data of the binary PPO/water phase diagram (see ref 16). [c] From the fit to the experimental data of the ternary PEO/PPO/water phase diagram (see ref 19).

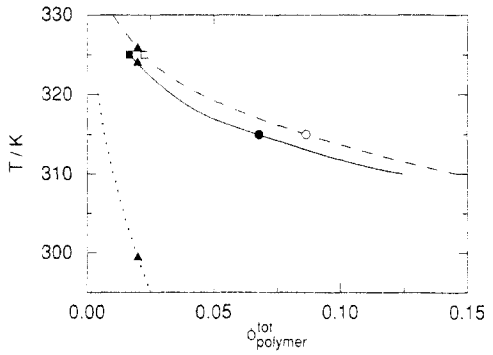

Figure 3. Critical micellar temperature (T) for aqueous solutions of a Pluronic P105–diblock mixture with $x^{tot}_{diblock} = 0.05$ (solid curve), of Pluronic P105 (dashed curve), and of the diblock copolymer (dotted curve) as a function of the total polymer volume fraction ($\phi^{tot}_{polymer}$). The symbols indicate conditions considered further below.

other Pluronic polymers,[11,12] the critical micellar concentration (cmc) depends strongly on the temperature. The diblock impurity considered, $(EO)_{37}(PO)_{56}$, has also an amphiphilic character and is able to form micelles on its own in solution. Figure 3 (dotted curve) shows that the cmc for an aqueous solution of the diblock copolymer (for a given temperature) is strongly reduced as compared with the cmc for an aqueous solution of Pluronic P105. The lower cmc of the diblock copolymer is a consequence of its more hydrophobic character. In addition, the requirement of only having one EO–PO junction per chain (instead of two) localized to the hydrophobic–hydrophilic interfacial region in the micelles facilitates the micellization.[11]

In the experimental situation, a small, but often unknown, fraction of the polymer content exists as diblock copolymers. Figure 3 shows that for a diblock impurity constituting 5% of the total polymer content, i.e., $x^{tot}_{diblock} \equiv \phi^{tot}_{diblock}/\phi^{tot}_{polymer} = 0.05$, where $\phi^{tot}_{polymer} = \phi^{tot}_{P105} + \phi^{tot}_{diblock}$ is the total polymer concentration, the cmc is reduced by ≈20–30% (cf. solid and dashed curves) or alternatively the cmt is reduced by some Kelvin. Since the amount of diblock impurity is most likely to be less than 5% of the polymer content, the model calculations predict that the occurrence of diblock impurities only marginally affects the cmc. However, as will be shown later, other properties are more strongly affected by the presence of diblock impurities. Thus, depending on the technique used to monitor the cmc, the change in the cmc due to the presence of diblock impurities in the solution could be essential in the experimental case.

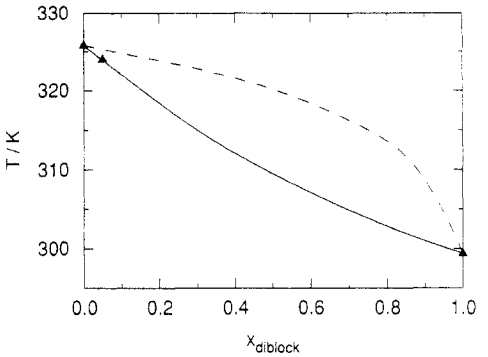

Figure 4. Critical micellar temperature (T) for an aqueous solution of a Pluronic P105–diblock mixture as a function of the fraction of diblock copolymer ($x^{tot}_{diblock}$) (solid curve) at a total polymer volume fraction $\phi^{tot}_{polymer} = 0.02$. The volume fractions of diblock copolymer in the micelles ($x^{mic}_{diblock}$) at the critical micellar temperatures are also given (dashed curve). The filled triangles here and in Figure 3 denote pairwise identical systems and conditions.

Figure 4 shows the cmt for an aqueous solution of a Pluronic P105–diblock mixture as a function of the diblock copolymer fraction of the total polymer amount, $x^{tot}_{diblock}$, at a fixed total polymer volume fraction of $\phi^{tot}_{polymer} = 0.02$ (solid curve). The depression of the cmt depends linearly on the diblock copolymer fraction up to $x^{tot}_{diblock} \approx 0.3$, and it levels slightly off at higher $x^{tot}_{diblock}$. Thus, the model suggests that the reduction of the cmt is essentially proportional to the polymer fraction of the diblock impurity. Also displayed in Figure 4 is the volume fraction of the polymer content in the micelles which is constituted by diblock copolymers, $x^{mic}_{diblock} \equiv \Gamma_{diblock}/\Gamma_{polymer}$, where $\Gamma_{polymer} = \Gamma_{P105} + \Gamma_{diblock}$ (dashed curve). The location of the $x^{mic}_{diblock}$ curve above the $x^{tot}_{diblock}$ curve implies a preferential micellization of the diblock copolymer. The increase of the diblock copolymer fraction in the micelle as compared with the diblock copolymer fraction of the whole system can be expressed by the ratio $x^{mic}_{diblock}/x^{tot}_{diblock}$. The maximal ratio occurs as $x^{tot}_{diblock}$ approaches zero, and the ratio is reduced with increasing $x^{tot}_{diblock}$ with the limiting value of 1. For the case shown in Figure 4, the maximal ratio is 4.3, and for the 5% diblock impurity case previously considered, 20% of the volume of the aggregated polymer is constituted by diblock copolymers, i.e., $x^{mic}_{diblock}/x^{tot}_{diblock} = 4.0$. The preferential micellization of the more hydrophobic diblock impurity is most prominent close to the cmc, and it reduces as the total polymer concentration increases (see Figure 7 below).

Figure 5 shows total polymer volume fractions as a function of the radial distance from the center of the micelle for a total polymer volume fraction $\phi^{tot}_{polymer} = 0.0225$ at $T = 325$ K (corresponding to the open square in Figure 3). The volume fractions at large layer numbers correspond to bulk values. Total *polymer* volume fraction profiles are given for a 5% diblock impurity (full curve) and for a pure Pluronic P105 solution (dashed curve). The conditions were selected such that the pure Pluronic P105 solution is at the cmc (open square in Figure 3) and consequently the solution with diblock impurity is slightly above *its* cmc (filled square in Figure 3). From Figure 5 it is inferred that the presence of the diblock impurity increases the micellar size by extending the micellar core (the region with constant polymer volume fraction) further

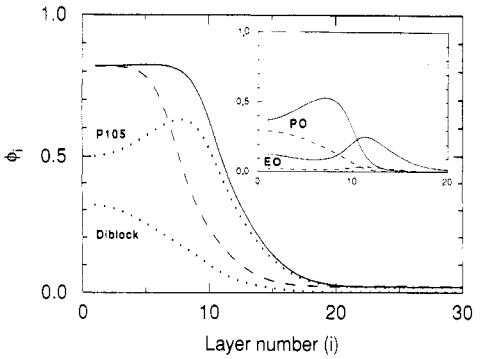

Figure 5. Total polymer volume fraction ($\phi_{\text{polymer},i}$) as a function of layer number (i) for an aqueous solution of a P105–diblock mixture with $x^{\text{tot}}_{\text{diblock}} = 0.05$ (solid curve) and for an aqueous solution of P105 (dashed curve), both with a total polymer volume fraction $\phi^{\text{tot}}_{\text{polymer}} = 0.0225$ at $T = 325$ K. For the mixture, the total volume fractions of Pluronic P105 ($\phi_{\text{P105},i}$) and diblock copolymer ($\phi_{\text{diblock},i}$) as a function of layer number (i) are also shown (dotted curves). The selected polymer volume fraction and temperature corresponds to the open square in Figure 3. Inset: Total segment volume fraction of Pluronic P105 ($\phi_{\text{EO(P105)},i}$ and $\phi_{\text{PO(P105)},i}$) (solid curves) and of diblock copolymer ($\phi_{\text{EO(diblock)},i}$ and $\phi_{\text{PO(diblock)},i}$) (dashed curves) as a function of layer number (i) for the aqueous solution of the P105–diblock mixture.

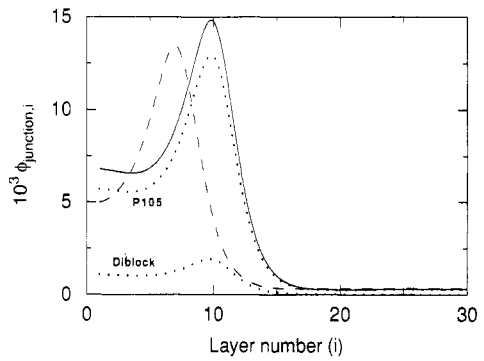

Figure 6. Total volume fraction of the EO–PO junctions ($\phi_{\text{junction},i}$) as a function of layer number (i). Conditions and symbols as in Figure 5.

out. The effective aggregation number increases from 18.9 to 46.6, of which 38.1 are Pluronic P105 polymers and the rest formed by 12.0 diblock copolymers. The separate density profiles of Pluronic P105 and the diblock copolymer are also given in Figure 5. It is seen that the diblock copolymer is preferentially located in the central part of the micelle, whereas the volume fraction of Pluronic P105 is substantially reduced in the micellar center, as compared with the case of no impurities (dashed curve). This replacement of Pluronic P105 with diblock copolymer leads to a maximum of the Pluronic P105 density, here in layer 8.

The volume fraction profiles of the EO and PO segments of Pluronic P105 and of the diblock impurity are shown by the inset in Figure 5. The EO profiles are nearly proportional; the difference in magnitude reflects the lower content of diblock copolymer in the micelles, $x^{\text{mic}}_{\text{diblock}} = 0.18$, and the lower fraction of EO in the diblock copolymer than in Pluronic P105 (see Figure 2). On the other hand, the distributions of the PO segments differ in character. The PO segments of the diblock copolymer are preferred to be closer to the center of the micellar core, whereas the PO segments of Pluronic P105 form an outer shell of the core.

In addition to the segment profiles, the model calculations also provide information on the spatial location of the EO–PO junctions (cf. eq 3). Figure 6 shows the volume fraction profile of the EO–PO junctions for the cases

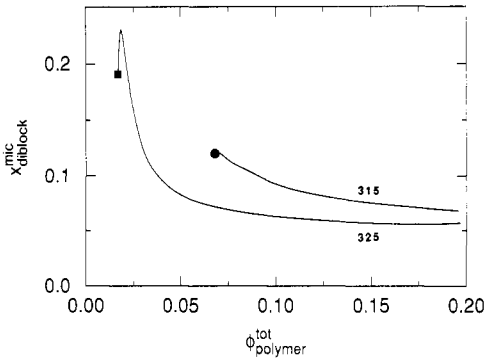

Figure 7. Fraction of diblock copolymer ($x^{\text{mic}}_{\text{diblock}}$) in micelles for an aqueous solution of a Pluronic P105–diblock mixture with $x^{\text{tot}}_{\text{diblock}} = 0.05$ as a function of the total polymer volume fraction ($\phi^{\text{tot}}_{\text{polymer}}$) at $T = 315$ and 325 K. The symbols denote the cmc, and the corresponding symbols in Figure 3 denote identical systems and conditions.

considered in Figure 5. The location of the maxima of the junction distributions corresponds to the border between the EO- and PO-rich domains (cf. inset of Figure 5). Although clear maxima are present, the distributions of the junctions are broad and the volume fractions of the junctions are appreciable in the centers of the aggregates. The presence of the diblock impurity does not change the extension of the zone of EO–PO junctions for Pluronic P105. Moreover, the volume fraction curves of the junctions for Pluronic P105 and for the diblock impurity (dotted curves) are almost proportional to each other. The unequal distributions of the PO segments (Figure 5, inset) and the proportional PEO–PPO junction distributions imply that the PPO block of the diblock copolymer is more stretched than the PPO block of the triblock copolymer. Thus, the occurrence of diblock impurities *does not* lead to a reduction of the EO–PO contacts by a sharpening of the EO–PO interface and the distribution of the EO–PO junctions of the diblock copolymers is the *same* as that of the junctions of Pluronic P105 despite different molecular composition and block structure.

Next, we will consider how some quantities characterizing the micelles vary with the total polymer volume fraction at 315 and 325 K for an aqueous solution of Pluronic P105 with and without diblock impurity. Thus, we will monitor the consequences of a small amount of diblock impurity. Again a diblock impurity of 5% of the total polymer content, i.e., $x^{\text{tot}}_{\text{diblock}} = 0.05$, will be considered.

Figure 7 shows the fraction of diblock copolymer in the micelles as a function of the total polymer volume fraction between the cmc and 0.2 at the two temperatures. Generally, the preferential aggregation of the diblock copolymer decreases with the total polymer volume fraction. However, the maximum of $x^{\text{mic}}_{\text{diblock}}$ occurs at a total polymer volume fraction slightly larger than the cmc (the shift from the cmc increases with the temperature, and the origin of the shift will be discussed below). Well above the cmc, the diblock/P105 ratio in the micelle becomes close to that in solution. Another observation is that the relative amount of diblock copolymer in the micelle increases at reducing temperature at a given, but sufficient large, total polymer volume fraction. The relative concentration of the free diblock impurity in the solution, i.e., $\phi^{\text{f}}_{\text{diblock}}/\phi^{\text{tot}}_{\text{diblock}}$, increases slower than the relative concentration of free Pluronic P105 at reducing temperature, and hence the micelles become relatively richer in the diblock impurity.

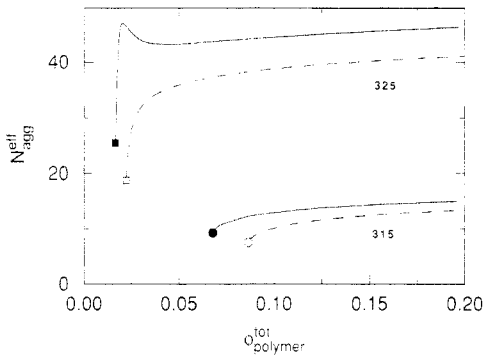

Figure 8. Effective micellar aggregation number (N_{agg}^{eff}) for an aqueous solution of a Pluronic P105–diblock mixture with $x_{diblock}^{tot} = 0.05$ (solid curves) and of Pluronic P105 (dashed curves) as a function of the total polymer volume fraction ($\phi_{polymer}^{tot}$) at T = 315 and 325 K. The symbols denote the cmc, and the corresponding symbols in Figure 3 denote identical systems and conditions.

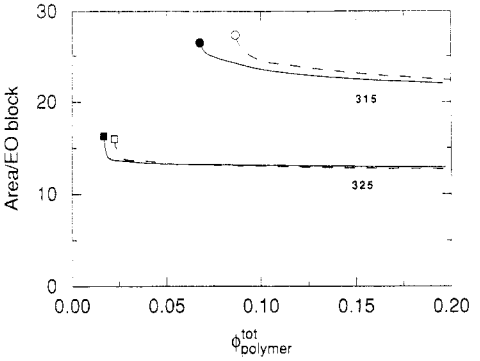

Figure 9. Headgroup area per PEO block, in lattice units, for an aqueous solution of a Pluronic P105–diblock mixture with $x_{diblock}^{tot} = 0.05$ (solid curves) and of Pluronic P105 (dashed curves) as a function of the total polymer volume fraction ($\phi_{polymer}^{tot}$) at T = 315 and 325 K. See text for the definition of the headgroup area. The symbols denote the cmc, and the corresponding symbols in Figure 3 denote identical systems and conditions.

Not only the cmc but also the aggregation number of the Pluronic micelles are strongly sensitive to the temperature. Figure 8 shows that the aggregation number of micelles formed in pure Pluronic P105 solution increases from 8 to 12 at increasing polymer concentration at 315 K, whereas the aggregation number at the cmc is ≈20 at 325 K and increases to ≈40 at higher total polymer concentration. In the presence of 5% diblock impurity, the effective aggregation number becomes larger. At the higher temperature and at increasing total polymer concentration, the effective aggregation number increases rapidly and displays a maximum at $\phi_{polymer}^{tot} \approx 0.02$, similar volume fraction at which $x_{diblock}^{mic}$ displayed its maximum. Well above the cmc, the effective aggregation number becomes independent of the total polymer volume fraction, and it becomes ca. 10–15% larger than the aggregation number without impurity. The calculated hydrodynamic radius displays a similar dependence on impurity, temperature, and the total polymer volume fraction.

If only one aggregating component were present (e.g., Pluronic P105 polymers without diblock impurity), the aggregation number increases monotonically with the total polymer concentration for stability reasons.[11,15] This condition is not applicable for the effective aggregation number in a system where several components aggregate. In Figure 8, the maximum displayed at 325 K is entirely due to the fact that the number of diblock copolymers per micelle as a function of the total polymer concentration displays a maximum. The number of Pluronic P105 polymers in the micelles increases monotonically with the total polymer concentration.

The reason for the existence of a maximum of $x_{diblock}^{mic}$ and of the number of aggregated diblock copolymers per micelle is as follows. The relative amount of aggregated diblock copolymers, i.e., $(\phi_{diblock}^{tot} - \phi_{diblock}^{f})/\phi_{diblock}^{tot}$, and of aggregated Pluronic P105 polymers, $(\phi_{P105}^{tot} - \phi_{P105}^{f})/\phi_{P105}^{tot}$, increases with $\phi_{polymer}^{tot}$. Since $\phi_{P105}^{tot} \gg \phi_{diblock}^{tot}$, normally $\phi_{P105}^{tot} - \phi_{P105}^{f}$ increases faster than $\phi_{diblock}^{tot} - \phi_{diblock}^{f}$ with $\phi_{polymer}^{tot}$. However, just after the cmc the reverse occurs, since the diblock copolymer is the least soluble of the two copolymers, and hence $x_{diblock}^{mic}$ display a maximum as a function of the total polymer volume fraction. Because the number of Pluronic P105 copolymers per micelle increases with $\phi_{polymer}^{tot}$, the peak in the effective aggregation number is shifted to larger $\phi_{polymer}^{tot}$ and is less prominent (or is even absent) as compared with $x_{diblock}^{mic}$. The occurrence of the maxima becomes more pronounced at increasing temperature, since the difference in solubility becomes more accentuated.

The growth of spherical micelles formed by nonionic surfactants [alkyl chain with an oligo(ethylene oxide) headgroup] at elevated temperature is normally attributed to a smaller repulsion among the headgroups, which is a consequence of a reduction of the extension of the headgroups due to poorer solvency condition.[20] In Figure 9, the projected headgroup area per EO block is given as a function of the total polymer concentration at the two temperatures. The locations of the peaks of the Pluronic EO–PO junctions (see Figure 6) were taken as radii of the spheres for the projection. Indeed, Figure 9 shows that the headgroup area reduces drastically at increasing temperature but that the headgroup area is essentially *independent* of the presence of diblock impurity and of the total polymer concentration. This fact, in conjunction with finding that the effective aggregation number is only weakly dependent on the presence of diblock impurity and of the total polymer concentration, supports that the aggregation number is strongly controlled by the interactions among the headgroups in this system as well. Finally, using a lattice length of 4 Å,[11] the area per EO block would be ≈370 Å² at 315 K and 210 Å² at 325 K.

To conclude, the presence of a small fraction of diblock impurities reduces the cmc by ≈20–30% or alternatively reduces the cmt by a few Kelvin. The reduction of the cmt is nearly proportional to the amount of diblock impurity present. More important, however, is the increase of the micellar aggregation number and size. The fact that the presence of diblock copolymer does not change the headgroup area as well as the similar EO–PO junction distributions and EO distributions of Pluronic P105 and diblock impurity strongly supports that the diblock copolymers are integrated into the micelles in a way similar to that of the Pluronic polymers. The main exception is the distribution of the PO segments. Hence, the growth of the micellar size, when the diblock copolymers are incorporated into the micelles, has to be attributed directly to the diblock copolymer having only one PEO headgroup, as compared with two for the Pluronic polymers. This causes a reduction of the optimal curvature by an enlargement of the core without making the repulsion among headgroups more severe.

PPO Impurity. The solubility of the $(PO)_{56}$ homopolymer in pure water is small, on the order $\phi_{PPO} = 10^{-5}$–10^{-4}, and the PPO homopolymer is strongly solubilized in the micelles. The presence of a PPO impurity

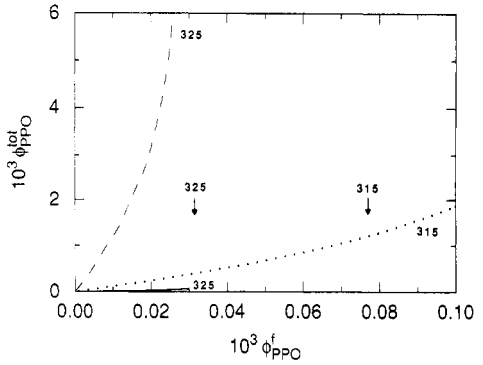

Figure 10. Total volume fraction of PPO homopolymer (ϕ^{tot}_{PPO}) as a function of free volume fraction of the PPO homopolymer (ϕ^{f}_{PPO}) for an aqueous solution of a P105–PPO mixture at a total P105 volume fraction of $\phi^{tot}_{P105} = 0.0225$ at $T = 325$ K (at cmc without PPO; solid curve), $\phi^{tot}_{P105} = 0.10$ at $T = 325$ K (above cmc without PPO; dashed curve), and $\phi^{tot}_{P105} = 0.10$ at $T = 315$ K (close to cmc without PPO; dotted curve). The solubility of PPO in pure water at $T = 315$ and 325 K is indicated with arrows.

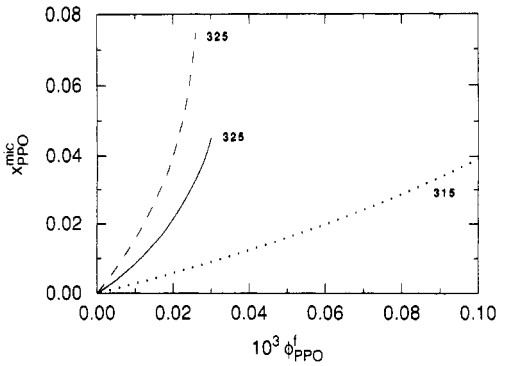

Figure 11. Fraction of PPO homopolymer (x^{mic}_{PPO}) in micelles as a function of the free volume fraction of the PPO homopolymer (ϕ^{f}_{PPO}) for an aqueous solution of a P105–PPO mixture. Conditions and meanings of the curves are as in Figure 10.

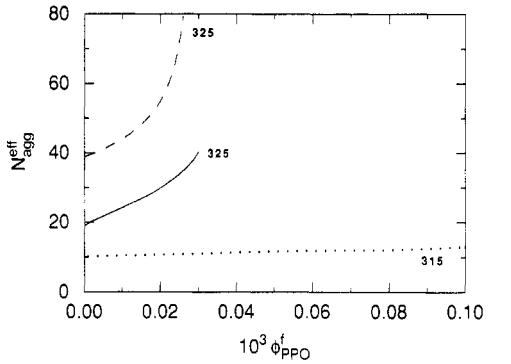

Figure 12. Effective micellar aggregation number (N^{eff}_{agg}) as a function of the free volume fraction of the PPO homopolymer (ϕ^{f}_{PPO}) for an aqueous solution of a P105–PPO mixture. Conditions and meanings of the curves are as in Figure 10.

suppresses the cmc by 5% at 325 K and 15% at 315 K at the solubility limit of PPO in the aqueous solution of Pluronic P105.

The most interesting aspect of the occurrence of a PPO homopolymer is its solubilization in the Pluronic polymer micelles. In order to discuss the solubility, it is useful to consider the volume fraction of free PPO as an independent variable rather than the fraction of the polymer impurity. The volume fraction of free PPO is directly related to the chemical potential of PPO.

Figure 10 shows the total volume fraction of PPO as a function of the free volume fraction of PPO at (T/K, ϕ^{tot}_{P105}) = (325, 0.0225), (325, 0.10), and (315, 0.10). The cases selected would, in the absence of PPO impurity, correspond to the cmc, well above the cmc, and close to the cmc, respectively (cf. Figure 3). The solubilization of PPO causes a dramatic increase of the dissolving capacity of PPO in aqueous solution. Since $\phi^{f}_{PPO} \ll \phi^{tot}_{PPO}$, almost all PPO is solubilized in the Pluronic polymer micelles. The total amount of PPO increases nearly exponentially with the free PPO concentration, albeit the exponential coefficient differs strongly among the cases. Moreover, the total amount of PPO increases with temperature at a constant volume fraction of Pluronic P105 and increases strongly with the volume fraction of Pluronic P105 at constant temperature. The strong dependence of the solubility on the Pluronic concentration is due to both a change of the solubilization capacity of individual micelles and a change of the micellar number density. At the cmc, the dissolving capacity of PPO is restricted since the micellar number density is low. A 4-fold increase of the total Pluronic P105 volume fraction (from 0.0225 to 0.10) at $T = 325$ K enhances the dissolving capacity [$\phi^{tot}_{PPO}/\phi^{f}_{PPO}$(saturation)] 200-fold.

The upper ends of the solubilization curves cease at the solubility limit of free PPO (higher PPO volume fraction would lead to phase separation). At 315 K, the solubility limit is $\phi^{f}_{PPO} = 1.0 \times 10^{-4}$, which is *larger* than the corresponding limit in pure water 7.7×10^{-5}, whereas at 325 K and the limits 3.0×10^{-5} and 2.6×10^{-5} for $\phi^{tot}_{P105} = 0.0225$ and 0.10, respectively, are *smaller* than the corresponding one in pure water 3.1×10^{-5}. At low temperature, as in the former case, the solubility limit of free PPO is increased since the intermicellar solution becomes more hydrophobic by the presence of a small amount of Pluronic P105. At higher temperature, the pure Pluronic P105 solution becomes less stable with respect to phase separation.[21] At 325 K, the stability of the pure Pluronic P105 solution is sufficiently low that an addition of PPO, equivalent to its solubility limit in pure water, causes a phase separation.

Despite the relatively low total volume fraction of PPO in the system, $\phi^{tot}_{PPO} \leq 0.006$, the strong solubilization makes the polymer volume fraction of PPO substantial in the micelles. Figure 11 shows that x^{mic}_{PPO} (similarly defined as $x^{mic}_{diblock}$) grows rapidly with increasing ϕ^{f}_{PPO}, and at the higher volume fraction at 325 K, up to ≈7% of the micellar volume consists of PPO. Also concluded from Figure 11 is that x^{mic}_{PPO} depends only weakly on the Pluronic P105 concentration but strongly on the temperature. At $\phi^{tot}_{P105} = 0.10$, a 10 K increase enhances the fraction of PPO in the micelles by an order of magnitude (cf. dashed and dotted curves).

Figure 12 displays the effective aggregation number for the same conditions as in Figure 11. The intercepts at $\phi^{f}_{PPO} = 0$ correspond to the aggregation numbers in the absence of PPO. These aggregation numbers increase with the total volume fraction of Pluronic P105 and temperature, which has been discussed previously.[11] The figure shows that, at the lower temperature, the increase of the effective aggregation number with ϕ^{f}_{PPO} is weak, whereas at the higher temperature a strong increase is obtained. The enlargement of the micelles is due to an increase *both* of the number of P105 polymers and of the number of PPO chains per micelle. The increase of the effective aggregation number for the two different ϕ^{tot}_{P105} at 325 K is almost parallel, indicating a micellar growth indepenent of ϕ^{tot}_{P105}. A comparison of Figures 11 and 12 shows that

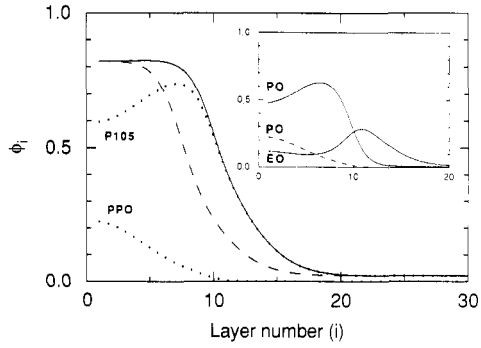

Figure 13. Total polymer volume fraction ($\phi_{\text{polymer},i}$) as a function of layer number (i) for an aqueous solution of a P105–PPO mixture with $\phi^{\text{tot}}_{\text{PPO}} = 6.7 \times 10^{-5}$ (solid curve) and for an aqueous solution of P105 (dashed curve), both with a total polymer volume fraction $\phi^{\text{tot}}_{\text{polymer}} = 0.0225$ at $T = 325$ K. For the mixture, the total volume fractions of Pluronic P105 ($\phi_{\text{P105},i}$) and PPO polymer ($\phi_{\text{PPO},i}$) as a function of layer number (i) are also shown (dotted curves). The selected polymer volume fraction and temperature corresponds to the open square in Figure 3. Inset: Total segment volume fraction of Pluronic P105 ($\phi_{\text{EO(P105)},i}$ and $\phi_{\text{PO(P105)},i}$) (solid curves) and of the PPO homopolymer ($\phi_{\text{PO(PPO)},i}$) (dashed curve) as a function of layer number (i) for the aqueous solution of the P105–PPO mixture.

there is a strong correlation between the fraction of PPO in the micelle and the increase of the aggregation number.

Volume fraction profiles for $\phi^{\text{tot}}_{\text{P105}} = 0.0225$ at $T = 325$ K with the maximal amount of PPO solubilized, $\phi^{\text{tot}}_{\text{PPO}} = 6.7 \times 10^{-5}$, are shown in Figure 13. The micelle consists of 38.5 Pluronic P105 polymers and 4.3 PPO homopolymer chains, giving an effective aggregation number of 40.3. The total polymer volume fraction profiles resemble closely those in Figure 5, which were for the same total polymer concentration and tempertaure but with the diblock instead of the PPO impurity. However, the total volume fraction of the PPO impurity is $\phi^{\text{tot}}_{\text{PPO}} = 0.067 \times 10^{-3}$ as compared with $\phi^{\text{tot}}_{\text{diblock}} = 1.1 \times 10^{-3}$, a 17-fold difference. The inset of Figure 13 shows that the PO segments of Pluronic P105 are similarly partly withdrawn from the center of the micelle. As for the diblock case, the localization of the PO segments of the PPO homopolymer to the center of the core releases stretching free energy of the PPO block of the Pluronic polymer. A closer inspection of Figures 5 and 13 shows that the PO segments of PPO are somewhat stronger localized to the center of the micelle, as compared with the PO segments of the PPO–PEO diblock copolymer, in accord with the different numbers of PEO headgroups.

The headgroup areas remain virtually independent of $\phi^{\text{f}}_{\text{PPO}}$ and hence also independent of the total amount of PPO solubilized (cf. Figure 10). The areas per PEO block are ≈15, 13, and 23 for (T/K, $\phi^{\text{tot}}_{\text{P105}}$) = (325, 0.0225), (325, 0.10), and (315, 0.10), respectively, and thus the headgroup area is strongly dependent on the temperature but only weakly dependent on the Pluronic P105 concentration. The areas are also very similar to those obtained for the presence of diblock copolymers at the corresponding temperatures (cf. Figure 9).

Thus, again, it is demonstrated that the growth of the micelles at constant temperture occurs with almost constant headgroup area. In the case of the diblock impurity, the growth of the micelles is restricted by the repulsion among the headgroups; as the micelles become larger, the area per headgroup is reduced for geometrical reasons. The addition of the diblock impurity just moves this limit to larger aggregation numbers. On the other hand, with the PPO impurity, the micelles normally grow by solubilization until the solubility limit of the more hydrophobic PPO impurity is reached.

In the experimental situation, the problem with the PPO homopolymer impurity should be more easily controlled as compared to the PEO–PPO diblock impurity. By reducing the temperature to below the cmt, the PPO homopolymer should separate out. The effect of the remaining volume fraction of PPO is normally too low to be significant.

Hurter and Hatton have in a related work investigated the micellization of Pluronic polymers and the solubilization of naphthalene in the micelles using the same theoretical approach.[12] They used essentially the same interaction parameters for the modeling of water and the Pluronic polymers, the main exception being a different set of EO–PO interaction parameters. The naphthalene was treated as a flexible oligomer. They made a detailed comparison of how the solubility depends on the composition of the Pluronic polymers and also obtained a strong solubilization of the hydrophobic solute in the micellar core. Also in agreement with the present results, they found that the micellar aggregation number depends very weakly on the volume fraction of the Pluronic polymer, whereas the increased solubility at higher Pluronic polymer concentrations was due to an increased number density of the micelles.

Cogan et al. have also performed similar mean-field lattice calculations modeling the micellization of PEO–polystyrene diblock copolymers in cyclopentane solution.[22] In this system the micellar core, consisting of PEO, may solubilize water. Although the individual values of the interaction parameters are different, it is, as here, the incompatibility between one of the blocks and the solvent which is the driving force of the micellization. A comparison between the results of the two model systems shows a number of similarities. First, the cmc is reduced and the aggregation number is increased upon the addition of the solubilizate and the largest effect occurs at the solubility limit. Also quantitatively similar volume fraction profiles for the solubilizate are obtained as well as similar reduction of the volume fraction of the lyophobic block in the center of the core. Thus, on the basis of the same mean-field theory but applied to models of different experimental systems, a similar picture emerges. The existing quantitative discrepancies are due to differences in interaction parameters, diblock versus triblock copolymer, and small molecule versus homopolymer as solubilizate.

PEO Impurity. The most hydrophilic impurity studied is the $(EO)_{37}$ homopolymer. Within the model, it is completely soluble in water at the temperatures considered. The presence of a 5% PEO impurity causes only a marginal effect on the micellization. The cmt curve given in Figure 3 is shifted upward a few tens of a Kelvin. Similarly, the structure of the micelles formed remains almost unaffected. The distribution of the additional EO segments is uniform in the entire system except for an expulsion from the micellar core. For example, at the conditions shown in Figure 5, $\phi^{\text{tot}}_{\text{polymer}} \approx 0.023$ and $T = 325$ K (dashed curve), but with $x^{\text{tot}}_{\text{PEO}} = 0.05$ instead of $x^{\text{tot}}_{\text{PEO}} = 0$, the volume fraction of the EO segments is 2×10^{-5} in the center of the micelle and reaches half its free volume fraction in layer 9.

V. Conclusions

The influence of polymer impurities on the micellization of a triblock copolymer consisting of EO and PO segments was investigated on the basis of a lattice theory for

heterogeneous systems. The inverse temperature behavior of aqueous PEO and PPO solutions was taken into account by allowing the polymer segments to adopt different states depending on the temperature and composition of the solution. By this approach, the effective segment–segment interaction becomes both concentration and temperature dependent. Most of the effects discussed depend critically on the existence of a temperature-dependent segment–segment interaction. All the interaction parameters employed were derived independently in previous investigations of the phase diagram of simpler systems, and thus no adjustable parameters are present.

The results show that the presence of diblock impurities reduces the critical micellar concentration, or alternatively reduces the critical micellar temperature at fixed polymer concentration. In addition, the micelles become larger and there is a preferential aggregation of the diblock copolymers. It was found that the EO–PO interface did not sharpen in the presence of diblock copolymers. Instead, it was concluded that the micellar growth is a consequence of the reduction of the number of headgroups per PPO block and the growth was limited by the required area of the PEO headgroups.

The presence of PPO impurities also leads to a reduction of the cmc. It was found that the PPO homopolymer is strongly solubilized in the micellar core. The solubility due to solubilization of PPO could be 2 orders of magnitude larger than the solubility in a pure aqueous solution, and the micelles swell until the solubility limit of PPO is reached. The PO segments of the PPO homopolymers as well as those of the PEO–PPO diblock copolymer were preferentially located in the center of the micellar core. Such a location partly releases stretching free energy of the PPO block of the triblock copolymer.

The cmc and the aggregation number are hardly affected at all by the presence of the PEO impurity. The PEO homopolymer is dissolved in the solvent and only to a smaller extent in the outer EO layer of the micelles.

The reduction of the cmt due to the presence of diblock impurities is not sufficient to match the discrepancy between experimental and theoretical cmt of ≈20–30 K.[11,13] If we consider Pluronic P105 and the diblock copolymer as two fractions of a polydisperse component, a 5% diblock impurity would lead to a polydispersity index of $M_m/M_n = 1.005$. In view of the fact that this number is considerably larger for commercial polymers, it is anticipated that the effect of the polydispersity on the micellization is larger than the effect of the presence of diblock impurities.

Acknowledgment. M. Malmsten is gratefully acknowledged for valuable comments on the manuscript. This work was supported by the Swedish Research Council for Engineering Science (TFR).

References and Notes

(1) Attwood, D.; Collett, J. H.; Tait, C. J. *Int. J. Pharm.* **1985**, *26*, 25.
(2) Zhou, A.; Chu, B. *Macromolecules* **1988**, *21*, 2548.
(3) Wanka, G.; Hoffmann, H.; Ulbricht, W. *Colloid Polym. Sci.* **1990**, *268*, 101.
(4) Almgren, M.; van Stam, J.; Lindblad, C.; Li, P.; Stilbs, P.; Bahadur, P. *J. Phys. Chem.* **1991**, *95*, 5677.
(5) Brown, W.; Schillén, K.; Hvidt, S. *J. Phys. Chem.* **1992**, *96*, 6038.
(6) Malmsten, M.; Lindman, B. *Macromolecules* **1992**, *25*, 5440.
(7) Hurter, P. N.; Hatton, T. A. *Langmuir* **1992**, *8*, 1291.
(8) Fleischer, G. *J. Phys. Chem.* **1993**, *97*, 517.
(9) Mortensen, K.; Brown, W. *Macromolecules* **1993**, *26*, 4128.
(10) Nagarajan, R.; Ganesh, K. *J. Chem. Phys.* **1989**, *90*, 5843.
(11) Linse, P. *Macromolecules* **1993**, *26*, 4437.
(12) Hurter, P. N.; Scheutjens, J. M. H. M.; Hatton, T. A. *Macromolecules* **1993**, *26*, 5030.
(13) Linse, P. *J. Phys. Chem.* **1993**, *97*, 13896.
(14) Scheutjens, J. M. H. M.; Fleer, G. J. *J. Phys. Chem.* **1979**, *83*, 1619; **1980**, *84*, 178.
(15) van Lent, B.; Scheutjens, J. M. H. M. *Macromolecules* **1989**, *22*, 1931.
(16) Linse, P.; Björling, M. *Macromolecules* **1991**, *24*, 6700.
(17) Karlström, G. *J. Phys. Chem.* **1985**, *89*, 4962.
(18) Björling, M.; Linse, P.; Karlström, G. *J. Phys. Chem.* **1990**, *94*, 471.
(19) Malmsten, M.; Linse, P.; Zhang, K.-W. *Macromolecules* **1993**, *26*, 2905.
(20) Puvvada, S.; Blankschtein, D. *J. Chem. Phys.* **1990**, *92*, 3710.
(21) At 325 K, the two (T, ϕ^t_{P105}) points are located closer to the binodal curve than the corresponding point at 315 K is; cf. Figures 14 and 15 of ref 11.
(22) Cogan, K. A.; Leermakers, F. A. M.; Gast, A. P. *Langmuir* **1992**, *8*, 429.